Available online at www.eccomasproceedia.org
Eccomas Proceedia COMPDYN (2025) 2462-2471

ECCOMAS
Proceedia

COMPDYN 2025
10th ECCOMAS Thematic Conference on
Computational Methods in Structural Dynamics and Earthquake Engineering
M. Papadrakakis, M. Fragiadakis (eds.)
Rhodes Island, Greece, 15-18 June 2025

COMPARATIVE EXPERIMENTAL AND NUMERICAL ANALYSIS OF THE IN-PLANE LATERAL CYCLIC BEHAVIOR OF CLAY BRICK AIR LIME-BASED MASONRY WALLS

Armando Zagaroli[1], Iwona Galman[1] and Jan Kubica[1]

[1] Department of Structural Engineering,

Faculty of Civil Engineering, Silesian University of Technology

ul. Akademicka 2A, 44-100 Gliwice, Poland

{Armando.Zagaroli, Iwona.Galman, jan.kubica}@polsl.pl

Abstract

The seismic behavior of masonry walls built with air lime-based mortars remains still insufficiently characterized, with a lack of experimental data and comparative numerical-experimental studies to accurately reproduce their response. The experimental results from two walls made of clay bricks and two mortars with two different amounts of air lime in the binder subjected to lateral cyclic pushover tests are shown. The response of FEM models based on a macro-modelling approach, where masonry is treated as homogeneous materials is compared with the experimental results. The latter shows a limited difference in the prediction of peak lateral strength, while ultimate displacements and therefore the displacement ductility remain inadequately predicted, as already evidenced in similar modelling approaches.

Keywords: Air lime-based masonry, lateral cyclic response, total strain crack model.

doi: 10.7712/120125.12581.25260

1 INTRODUCTION

Air lime-based mortars, once commonly used in masonry construction before cement became widespread, are still frequently found in existing and heritage masonry structures. In this context, the analysis of the masonry structural response has mainly focused on the physical, chemical and morphological properties of the mortars [1], more then on the mechanical feature, due to the low strength of these materials. Indeed, comparative evaluations of the properties have revealed differences between historic and modern mortars, particularly in terms of morphological porosity and chemical composition [2], contributing to the distinct mechanical responses observed in historical and modern mortars. Despite their relatively low strength, air lime-based mortars offer several advantages including enhanced workability, durability and reduced environmental impact [3]. Advantages that extend beyond their application in conservation and rehabilitation efforts [4] remain significant even today and deserve renewed attention, establishing them as a sustainable choice for modern construction practices as well. In this context, to promote the use of air lime mortars in modern applications, Ramesh et al. [5] adopted a holistic approach to evaluate the compressive and flexural strength of mortars. They tested 14 different lime-cement mixtures, with lime content in the binder ranging from 10% to 75% (by volume) and varying binder-to-aggregate ratios. Their study also established regression equations linking the mechanical properties to the air lime content in the binder. Recently, Zagaroli et al. [6] conducted studies on the mechanical characterization of two air lime-based mortars, with a particular focus on their tensile, flexural, and fracture energy properties.

From the perspective of masonry performance, the analysis of masonry constructed with these types of mortars is primarily based on small-scale studies [7]. Costigan & Pavia [8] investigated the relationship between the mechanical properties of hydraulic and air lime mortars and masonry, focusing on mortar and masonry compressive strength. Their study demonstrated that increasing the mortar strength does not necessarily lead to a higher masonry strength, as bond strength plays a crucial role. Ramesh et al. [9] conducted comparative experimental tests on three mortars with increasing air lime content and the masonry constructed with them. Their results indicate that a higher air lime content in the binder generally reduces compressive strength and elastic modulus while increasing peak axial deformation. Recently, Ramesh et al. [10] investigated the influence of air lime content in mortars on the lateral cyclic behavior of masonry. Their findings revealed that adding air lime to the binder has a relatively minor impact on the lateral structural performance of masonry under in-plane cyclic displacement. From a practical perspective, the study suggests that partially replacing cement with lime in masonry mortars does not compromise mechanical performance, promoting the use of more sustainable materials. However, experimental studies analyzing the seismic behavior of masonry walls constructed with air lime-based mortars remain limited. Further research and additional data are needed to better understand their performance within a displacement-based design approach [11]. In this context, most studies focus on analyzing the response of masonry built with hydraulic mortars, often to investigate specific historical cases. Messali et al. [12] examined the behavior of typical calcium silicate hydraulic lime brick masonry in light of the increasing seismic risk in northern Netherlands. Elghazouli et al. [13] investigated the behavior of hydraulic lime brick masonry under both dry and wet conditions, highlighting stiffness reductions of up to 20% and lateral strength decreases of 11% in wet walls compared to dry ones. Subsequently, Guo et al. [14] confirmed these findings through a micro-modeling approach that discretizes bricks, mortars, and interfaces. From a computational perspective, while continuous macro-models provide a balance between accuracy and computational efficiency for analyzing large-scale masonry elements compared to micro-models [15], also Falkiar et al. [16] attempted to study the compressive response of air lime-based brick masonry stack-bonded prisms and wallettes using a detailed micro-modeling approach.

In this study, the experimental results of two masonry walls subjected to lateral cyclic loads are shown. The walls are built with clay bricks and the only difference is related to the mortar mixes used for building them with one mix having a superior content of air lime in the binder. The experimental results in terms of cyclic response of lateral loads and horizontal displacement is given. Backbone curves are compared with a finite element model based on the total strain crack model existing the DIANA Fea software [17].

2 MATERIALS AND METHODS

Clay units and two air lime-based mortars are used for constructing the masonry walls. The study considers two mortar types with different air lime contents, varying the proportions of air lime in the binder. Specifically, the mortar mixes, referred to as MIX-1C1L6S and MIX-1C2L9S, have volumetric ratios of cement, lime, and sand of 1:1:6 and 1:2:9, respectively. For bedding samples, air lime CL90-S [18], cement CEM II / B-L 32.5 R [19], and siliceous sand are used. Comprehensive analysis of the mechanical properties of the mortars are furnished in Zagaroli et al. [6]. Clay units, supplied by Wienerberger Building Construction Company, were tested in compression, with the results of this analysis presented in Falkjar et al. [16]. The latter [16] also provide the results of masonry wallettes tested in compression according to EN 1052-1 [20], focusing on peak compressive strength, elastic modulus, and peak axial deformation. Table 1 presents a summary of the mechanical properties of the mortars. The mechanical properties of their corresponding masonries, where MAS-1C1L6S and MAS-1C2L9S refer to the masonry constructed with lower and higher air lime content, respectively, are given in Table 2.

Table 1: Mechanical properties of mortars and Masonry tested in Zagaroli et al. [6].

Properties	MIX-1C1L6S	MIX-1C2L9S
Compressive strength [21]	7.91 MPa (13.1%)	4.16 MPa (7.6 %)
Flexural strength [21]	2.21 MPa (16.2%)	1.23 MPa (11.2%)

Table 2: Mechanical properties of Masonry analyzed in Falkjar et al. [16].

Properties	MAS-1C1L6S	MAS-1C2L9S
Compressive strength [20]	8.40 (15.9)	6.98 (3.8)
Elastic modulus [20]	2501.0 (11.6)	2166.9 (26.6)

The lateral cyclic tests were conducted on walls measuring 1350 × 102 × 1759 mm. The test setup (Fig. 1) was designed to replicate double-bending boundary conditions, allowing horizontal movement at the top while constraining rotational movement. The walls were constructed directly on concrete beams measuring 250 × 250 mm. Another 250 × 250 mm concrete beam was then fixed to the top of the wall using fast-setting cement mortar and connected to an external steel frame through a hinge system for applying lateral loads. Additionally, steel rollers were incorporated at the top to facilitate horizontal movement, while a steel redistribution beam was used to apply vertical loads in the model. A lateral actuator with a 1000 kN capacity was used in load-controlled application, monitoring the top horizontal displacements at each load increment with linear variable displacement transducers (LVDTs).

Additionally, a digital image correlation (DIC) system was used to one side of the wall, enabling the software GOM Correlate to qualitatively assess crack development (Fig. 2). The imposed displacement history was chosen following the recommendations of FEMA-461 [22], with drift levels proportional to the wall heights and an increasing amplitude factor of 1.4, starting from a drift of 0.05% until failure. Two walls were tested, one for each mortar mix, after 28 days of curing under laboratory conditions. The impact of carbonation on the compressive strength improvement of air lime-based mortars was considered to have a limited effect on the mechanical properties of the masonry, as predicted by existing compressive strength models from the literature [23-24]. Prior to applying the lateral load, a vertical precompression was applied to the top of the elements and maintained constant throughout the test, corresponding to 30% of the compressive strength of the respective masonry samples. Tab. 3 presents the geometric properties and vertical loads applied to the masonry specimens, where HT-1C1L6S and HT-1C2L9S correspond to the tests on masonry made with lower (MIX-1C1L6S) and higher (MIX-1C2L9S) air lime-based mortars, respectively.

Figure 1: Test set-up.

Figure 2: Camera position for the DIC system.

Table 3: Test program of masonry walls with dimensions and vertical pre-compressive load P.

Test	Masonry type	Base [mm]	Height [mm]	Thickness [mm]	P [kN]
HT-1C1L6S	MAS-1C1L6S	1350	1759	102	347.01
HT-1C2L9S	MAS-1C2L9S	1350	1759	102	285.04

3 EXPERIMENTAL RESULTS

Experimental results on the lateral cyclic response are given in terms of horizontal load applied and horizontal displacements for masonry HT-1C1L6S and HT-1C2L9S in Fig. 3a and 3b, respectively. The wall constructed using mortar with the lowest air lime content in the binder (HT-1C1L6S) initially develops cracks at the center (Fig. 4a), which eventually progress into diagonal cracking by the end of the test. This behavior aligns with expectations due to the boundary conditions and the high level of pre-compressive load applied (Fig. 4b) [25]. The wall HT-1C2L9S, which contains a higher lime content in the binder, developed a central crack. Additionally, a flexural movement was observed at the base on opposite sides of the wall, characterized by opposing compression and tension cracks (Fig. 5a). Ultimately, the test concluded with diagonal shear failure (Fig. 5b). At this stage, a comparison of the compressive strength of the two mortars and their corresponding masonry structures with the base shear of the related walls is presented in Table 4. The results confirm the trends observed by Ramesh et al. [10], showing that a reduction of approximately 50% in mortar compressive strength, due to a higher lime content mix, corresponds to only a 7% decrease in base shear.

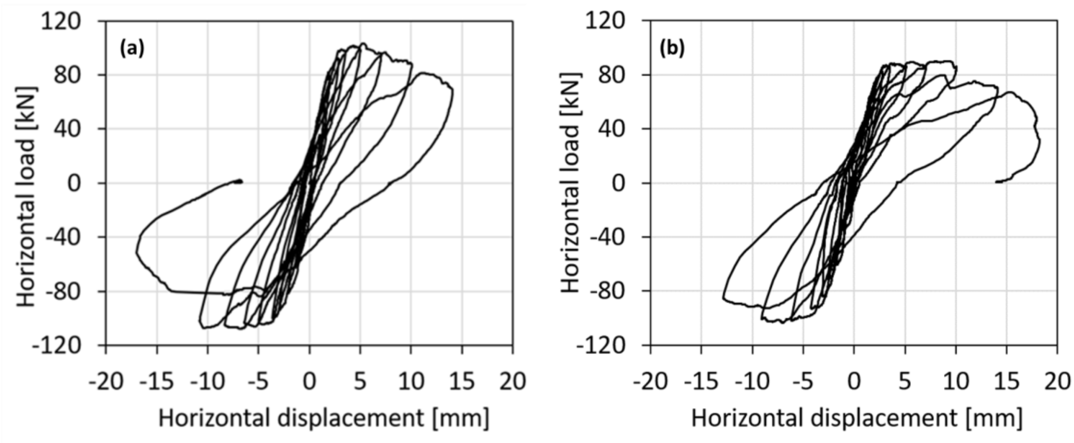

Figure 3: Experimental lateral load vs horizontal displacement for **a)** HT-1C1L6S and **b)** HT-1C2L9S.

4 NUMERICAL MODELLING

The numerical modelling of the response of the previously tested walls is conducted using a macro-modelling approach based on the Total Strain Crack (TSC) model in the DIANA software. This model uses a masonry constitutive stress-strain relationship to describe the deterioration caused by external loads, characterized by the formation of localized cracks while adhering to a continuity assumption. For this study, the rotating crack model was employed to use a "rotating" model, the crack orientation and the directions of principal stresses adjust dynamically with each load increment during the analysis. The calibration of the material models is based on analyzing the compressive stress-strain relationships obtained from wallettes tests [16], with additional parameters determined following the recommendations of Lourenco & Gaetani [26]. The input parameters for the TSC material model, which assumes a parabolic compression branch and an exponential softening branch in tension, are provided in Tab. 5.

These parameters include E (elastic modulus), ν (Poisson's ratio), f_m (masonry compressive strength), G_{fc} and G_{ft} (fracture energies in compression and tension, respectively), and f_t (masonry tensile strength).

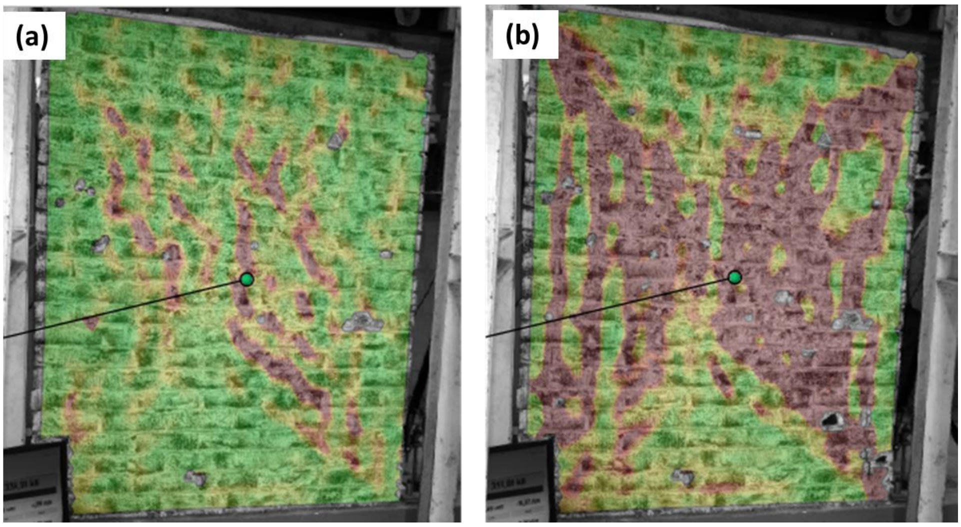

Figure 4: DIC crack patterns at **a)** first cracking **b)** and the end of the test for HT-1C1L6S.

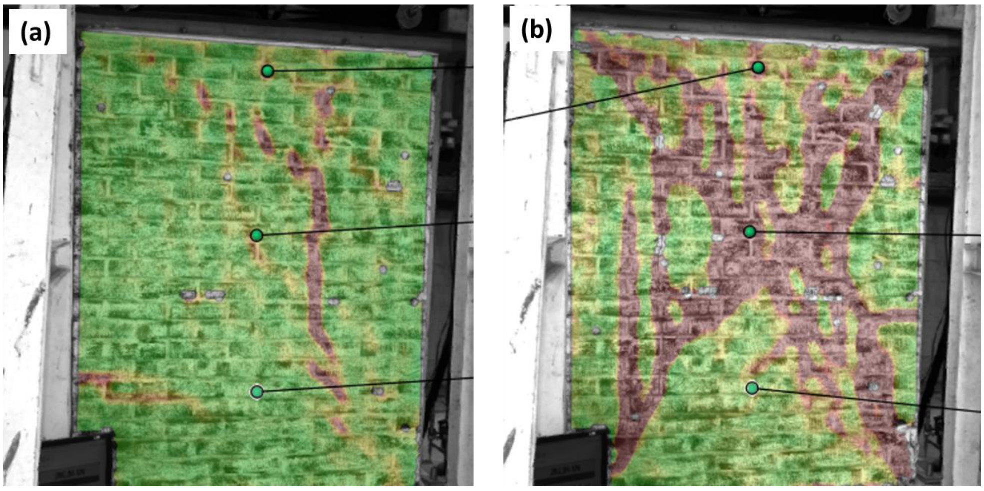

Figure 5: DIC crack patterns at **a)** first cracking **b)** and the end of the test for HT-1C2L9S.

Table 4: Average compressive strength of mortar f_{mix} and masonry f_m with average positive and negative peak base shear F_h from the cyclic tests.

Masonry type	f_{mix} [MPa]	f_m [MPa]	F_h [kN]
MAS-1C1L6S	7.91	8.40	99.84
MAS-1C2L9S	4.16	6.98	92.30
Diff [%]	47.41	16.90	7.55

Table 5: TSC parameters for macro-modeling of masonry material.

Masonry type	f_m [MPa]	E [MPa]	ν [-]	f_t [MPa]	G_{fc} [N/m]	G_{ft} [N/m]
MAS-1C1L6S	8.4	2500	0.19	0.4	11700	10
MAS-1C2L9S	6.9	2170	0.21	0.3	13200	20

Beyond the material properties, the FEM model (Fig. 6) utilizes plane stress elements with a four-point integration scheme with linear interpolation and a size of 10 × 10 mm. The top and bottom concrete beams are also modelled using the plane stress elements but with elastic isotropic material characterized by Young's modulus of 30 GPa and a Poisson's ratio of 0.2. The base of the model is restrained in both vertical and horizontal displacements. The top nodes of the wall are tied together to ensure uniform vertical and horizontal displacements, matching those at the point of lateral load application, in order to reproduce the double-clamped condition of the test. The lateral load is applied in force control with arc-length activated in order to obtain info on the post-peak behavior. Newton–Raphson method was chosen for equilibrium iterations, with convergence assessed based on the simultaneous satisfaction of energy and force criteria (set at 10^{-4} and 10^{-2}, respectively), and line search control enabled.

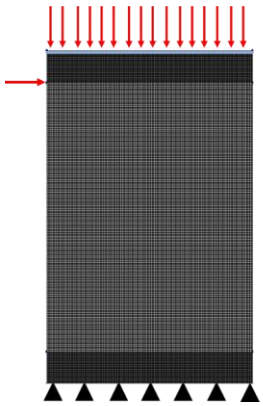

Figure 6: Finite element model for macro-modelling approach with vertical distributed load and horizontal load point evidenced (darker part represents concrete beams).

The comparison of the positive and negative backbone curves of the experimental lateral response with the numerical ones are given in Fig. 7a-b for the test HT-1C1L6S and Fig. 8a-b for HT-1C2L9S, respectively. The crack patterns of both walls at peak load, showing diagonal cracking, are given in Fig. 9a-b.

The models demonstrate a good match with experimental results in terms of stiffness across all cases. However, the peak lateral load is generally overestimated in the model, except in the case of masonry made with mortar HT-1C2L9S in the negative loading direction. For all the other cases, the overestimation ranges from about 3% to a 10% maximum, showing a reliable prediction for the peak strength. None of the models successfully capture the full softening behavior observed in the experimental tests. This limitation, particularly in predicting ultimate displacements for diagonal shear cracking, has been widely documented in the literature [26].

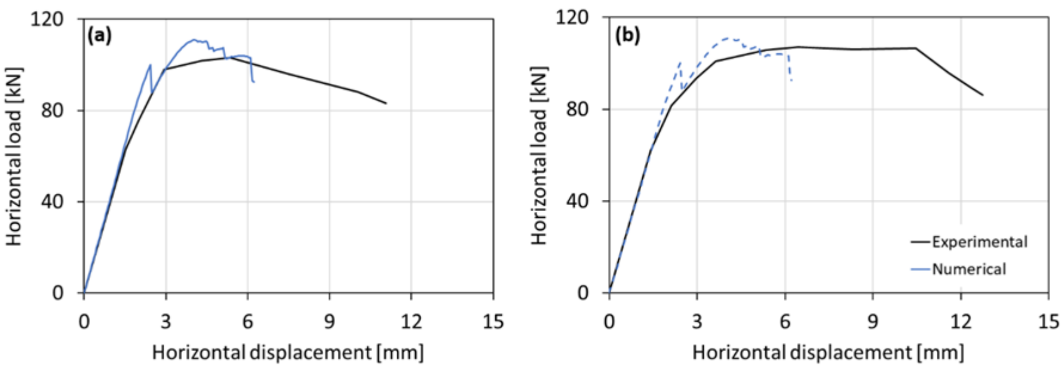

Figure 7: Experimental vs numerical lateral test results for **a)** positive and **b)** negative push direction for masonry made of HT-1C1L6S.

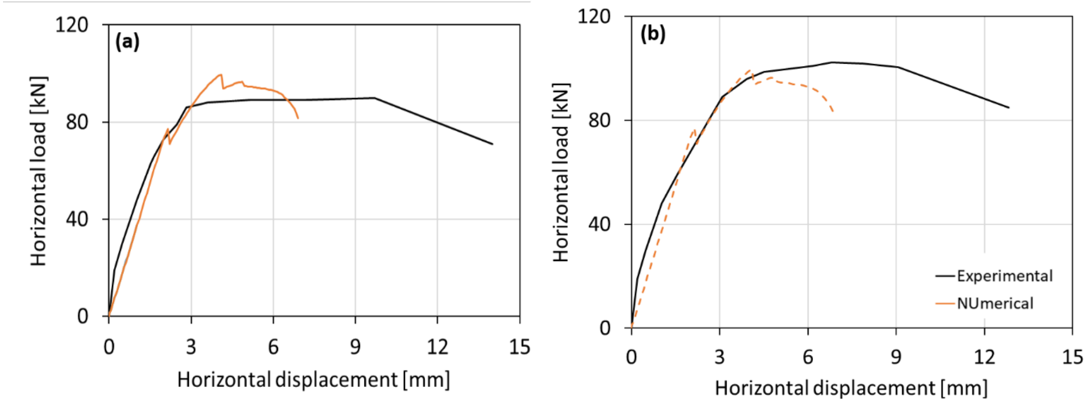

Figure 8: Experimental vs numerical lateral test results for **a)** positive and **b)** negative push direction for masonry made of HT-1C2L9S.

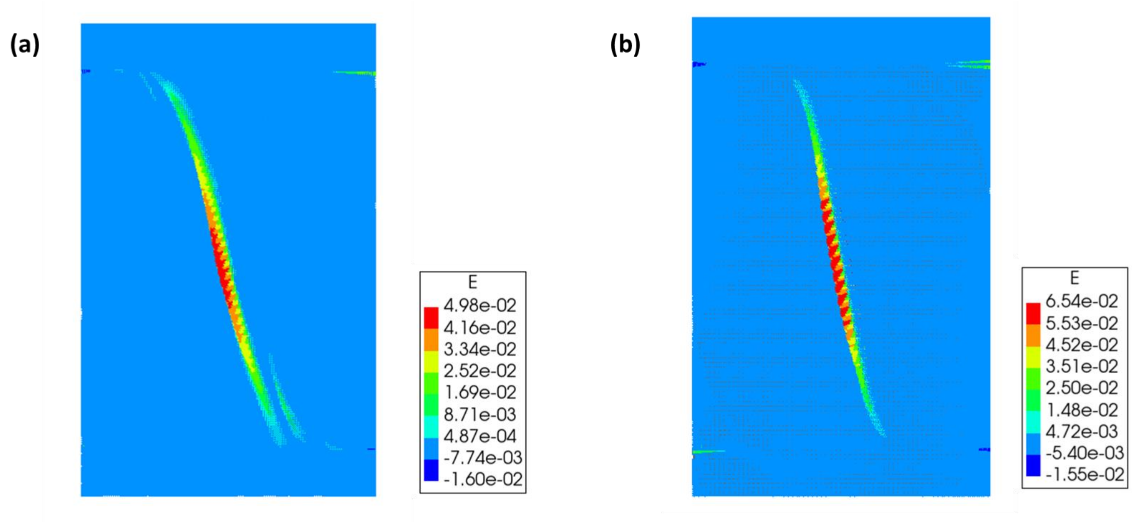

Figure 9: Principal crack strains at peak load for **a)** HT-1C1L6S and **b)** HT-1C2L9S.

Table 6: Masonry peak positive/negative horizontal load $F_h^{+/-}$ prediction and peak experimental strength with relative differences in positive and negative direction.

Masonry type	Fh-num [kN]	Fh^{+}-exp [kN]	Fh^{-}-exp [kN]	Diff^{+} [%]	Diff^{-} [%]
MAS-1C1L6S	110.84	103.10	107.21	6.99	3.28
MAS-1C2L9S	99.57	90.32	102.36	9.29	-2.80

5 CONCLUSION

Experimental tests were conducted on large-scale masonry walls subjected to lateral cyclic and vertical loads, utilizing two mortar mixes with varying air lime content, one of which contains double the volumetric amount of air lime in the binder. Numerical model based on a macro-modelling approach for masonry was adopted for a first assessment of the experimental results and a quick prediction of them. Results from the analysis show that:

- Although the mortar with a higher air lime content exhibits approximately 50% lower compressive strength, masonry constructed with the same mortar shows only a 7% average reduction in lateral shear strength. This indicates the potential viability of using high air lime content mortars for their sustainability advantages, despite not meeting the Eurocode 8 [27] requirement of a minimum compressive strength of 5 MPa.

- Simple macro-modelling approaches can reasonably predict the peak lateral of the tested masonry in horizontal loading; however, their accuracy in capturing post-peak behavior is limited, as already highlighted in previous studies.

REFERENCES

[1] Ergenç, D., Fort, R., Varas− Muriel, M.J. and Alvarez de Buergo, M., 2021. Mortars and plasters—How to characterize aerial mortars and plasters. Archaeological and Anthropological Sciences, 13(11), p.197.

[2] De Vico, F.S., Zagaroli, A., Rodríguez-Navarro, C., Kubica, J. and Gorski, M., 2023. A Physico-chemical Study of Lime-based Mortars from Different Historical Periods. NanoWorld J, 9(S2), pp.S256-S261.

[3] Campo, F.P., Tua, C., Biganzoli, L., Pantini, S. and Grosso, M., 2021. Natural and enhanced carbonation of lime in its different applications: a review. *Environmental Technology Reviews*, *10*(1), pp.224-237.

[4] Veiga, R., 2017. Air lime mortars: What else do we need to know to apply them in conservation and rehabilitation interventions? A review. Construction and Building Materials, 157, pp.132-140.

[5] Ramesh, M., Azenha, M. and Lourenço, P.B., 2019. Quantification of impact of lime on mechanical behaviour of lime cement blended mortars for bedding joints in masonry systems. *Construction and Building Materials*, *229*, p.116884.

[6] Zagaroli, A., Kubica, J., Galman, I. and Falkjar, K., 2024. Study on the Mechanical Properties of Two General-Purpose Cement–Lime Mortars Prepared Based on Air Lime. *Materials*, *17*(5), p.1001.

[7] Brando, G., Vacca, G., Di Michele, F., Capasso, I. and Spacone, E., 2022. Experimental and numerical mechanical characterization of unreinforced and reinforced masonry elements with weak air lime mortar joints. *Sustainability*, *14*(7), p.3990.

[8] Costigan, A. and Pavía, S., 2012. Influence of the mechanical properties of lime mortar on the strength of brick masonry. In *Historic Mortars: Characterisation, Assessment and Repair* (pp. 359-372). Dordrecht: Springer Netherlands.

[9] Ramesh, M., Parente, M., Azenha, M. and Lourenço, P.B., 2023. Influence of Lime on Strength of Structural Unreinforced Masonry: Toward Improved Sustainability in Masonry Mortars. *Sustainability*, *15*(21), p.15320.

[10] Ramesh, M., Ramirez, R., Azenha, M. and Lourenço, P.B., 2024. Evaluating the role of mortar composition on the cyclic behavior of unreinforced masonry shear walls. *Materials*, *17*(18), p.4443.

[11] Morandi, P., Albanesi, L., Graziotti, F., Piani, T.L., Penna, A. and Magenes, G., 2018. Development of a dataset on the in-plane experimental response of URM piers with bricks and blocks. *Construction and Building Materials*, *190*, pp.593-611.

[12] Messali, F., Esposito, R., Ravenshorst, G.J.P. and Rots, J.G., 2020. Experimental investigation of the in-plane cyclic behaviour of calcium silicate brick masonry walls. *Bulletin of Earthquake Engineering*, *18*(8), pp.3963-3994.

[13] Elghazouli, A.Y., Bompa, D.V., Mourad, S.A. and Elyamani, A., 2021. In-plane lateral cyclic behaviour of lime-mortar and clay-brick masonry walls in dry and wet conditions. *Bulletin of Earthquake Engineering*, *19*, pp.5525-5563.

[14] Guo, Y.T., Bompa, D.V. and Elghazouli, A.Y., 2022. Nonlinear numerical assessments for the in-plane response of historic masonry walls. *Engineering Structures*, *268*, p.114734.

[15] D'altri, A.M., Sarhosis, V., Milani, G., Rots, J., Cattari, S., Lagomarsino, S., Sacco, E., Tralli, A., Castellazzi, G. and De Miranda, S., 2020. Modeling strategies for the computational analysis of unreinforced masonry structures: review and classification. *Archives of computational methods in engineering*, *27*, pp.1153-1185.

[16] Falkjar, K., Zagaroli, A. and Kubica, J., 2024, July. Experimental Testing Versus Numerical Modelling of Small Masonry Wallettes in Axial Compression. In *International Brick and Block Masonry Conference* (pp. 412-431). Cham: Springer Nature Switzerland.

[17] Al-Chaar, G.K. and Mehrabi, A., 2008. Constitutive models for nonlinear finite element analysis of masonry prisms and infill walls.

[18] EN 459-1. (2010). Building lime: Definitions, specifications and conformity criteria–Part 1. CEN; Brussels.

[19] EN 197-1. (2011). Cement: Composition, specifications and conformity criteria for common cements–Part 1. CEN; Brussels.

[20] EN 1052-1. (2001) Part 1: Determination of compressive strength. CEN; Brussels.

[21] EN 1015-11. (2019) Part 11: Determination of flexural and compressive strength of hardened mortar. CEN; Brussels.

[22] Applied Technology Council, et al. Interim testing protocols for determining the seismic performance characteristics of structural and nonstructural components. Federal Emergency Management Agency, 2007.

[23] EN 1996-1-1: Eurocode 6. (2005). Design of masonry structures—Part 1-1: General rules for reinforced and unreinforced masonry structures. European Committee for Standardization (CEN).

[24] Kaushik, H.B., Rai, D.C. and Jain, S.K., 2007. Stress-strain characteristics of clay brick masonry under uniaxial compression. *Journal of materials in Civil Engineering*, *19*(9), pp.728-739.

[25] Magenes, G. and Calvi, G.M., 1997. In-plane seismic response of brick masonry walls. *Earthquake engineering & structural dynamics*, *26*(11), pp.1091-1112.

[26] Lourenço, Paulo B., and Angelo Gaetani. Finite element analysis for building assessment: Advanced use and practical recommendations. Routledge, 2022.

[27] EN 1998-3: Eurocode 8 (2005): Design of structures for earthquake resistance – Part 3: Assessment and retrofitting of buildings. European Committee for Standardization (CEN).